Applicability of local strength approaches for the fatigue assessment of welded vehicle components

Martin Vogt[a], Ekke Hanssen[a], Tim Welters[a], Klaus Dilger[a]

[a] Institute of Joining and Welding technology
Technical University of Braunschweig, 38106 Braunschweig, Germany

Abstract Within the scope of the research results presented here, the applicability of the structural and notch stress approach is under examination on the basis of different arc welded and dynamically loaded steel structures, taken from the automotive and railway sector. In detail these are a transverse control arm and a crossbeam connection from the underframe of a railcar body. Concerning the underframe of the car body, the crossbeam connections are the critical areas. Components and specimens with critical regions of failure are tested under dynamic loading with constant amplitude. With the help of strain gauges, the technical incipient crack is determined. The specimens are the basis for application and evaluation of the different concepts for the assessment of fatigue life. The numerical determination of the nominal, structural and notch stresses is performed with finite-element models. For a local approach, according to the notch stress analysis, a submodelling technique is used. Finally the experimental and computational results allow the derivation of structural and notch Woehler-lines (S-N-curves).

1 INTRODUCTION

For thin-walled steel structures the fatigue strength of weld seams is in many cases essential for the overall component strength, because the welded joints often turn out to be the weak spots of structures under dynamic loading with constant or variable amplitudes. The assessment of fatigue life allows, in an early point of design, a dimensioning of components appropriate for the expected working loads. Therefore well-defined and in terms of their prediction accuracy reviewed strength concepts are necessary.

The notch stress approach with a fictious notch radius r_f=1mm, is only defined in the IIW-Recommendation [01] and in the FKM-Guideline [02] and only applicable for thick steel plates with thicknesses of 5 mm or greater. Additionally components are partial loaded with variable amplitudes which results in the well known problems concerning the existing cumulative damage hypotheses with D=1 and the applicable strength criterion for multiaxial stress states [03]. So the different existing approaches have to investigate.

The results presented here are developed in the context of the research cluster "applicability of fatigue design concepts for dynamic loaded weld structures", which is promoted by the AiF. The applicability of the structural and notch stress approach on the basis of different arc welded steel structures is under examination. These are a transverse control arm (automotive sector) and a crossbeam connection from the underframe of a railcar body (railway sector).

The derivation of structural and notch Woehler-lines (S-N curves) is the aim of the experimental and computational results.

2 MATERIALS, SPECIMEN SHAPES AND TESTING METHOD

The crossbeam connections are the critical areas, concerning the underframe of the car body. The construction is build of u-profiles with different cross-sections and different sheet thicknesses. This leads within the region of the weld joints to an increase of stress. The construction steel S355J2G3 (1.0116) in a plate thickness of 3.0 mm and the fine grain cold pressure steel S500MC (1.0984) in a plate thickness of 4.0 mm are used for the investigation. To avoid testing a whole railcar body, different types of components and specimen are designed. The critical area of the crossbeam connection is the master for the different types of specimens and components (fig. 1). All specimens were manufactured by manual MAG-welding by the company ALSTOM LHB (Salzgitter, Germany). Component C (fig. 1) is a complex structure near the real railcar body, which will be tested under bending. A simplification of the crossbeam connection from the underframe of a railcar body with the load of component C, is the specimen B. It includes the different sheet thickness and the real welding seams, including the beginning and the end of the weld seam, as a combination of a butt and fillet joint. A further simplification of the critical area is built up in specimen A. The butt joint includes a misalignment of weld edges concerning the different sheet thicknesses (fig. 2). Specimen E is characteristic for a tensile loading of the longitudinal solebar, which is typical for the load in a railcar body.

In order to determine the fatigue strength behaviour, load-controlled test with constant amplitude and pulsating load (R = 0) were carried out with specimen A and B. For each specimen type 16 – 29 tests were carried out with a frequency of f = 30 Hz at room temperature in air. With the help of strain gauges, the technical incipient cracks were determined. The end of the test is defined by the fracture of the specimen or by 10^7.numbers of cycles. These results are the basis for application and evaluation of the different concepts for the assessment of fatigue life.

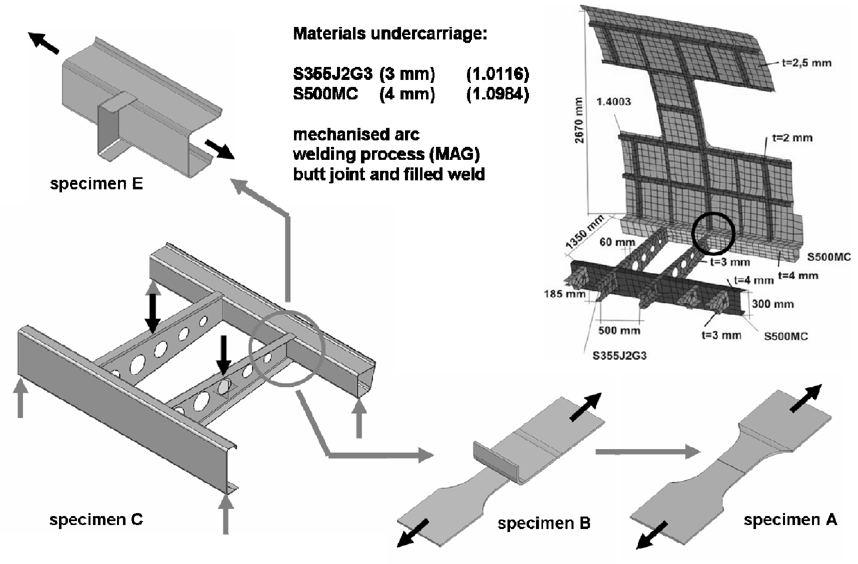

Figure 1. Specimens and components for fatigue tests

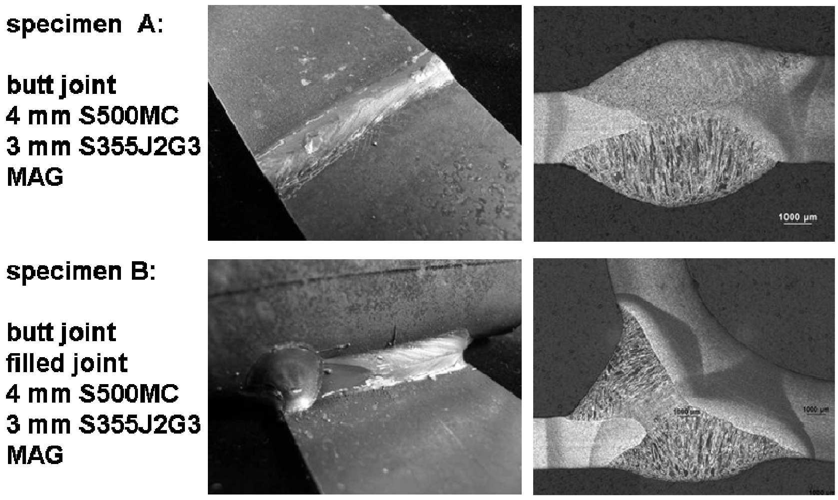

Figure. 2. Weld seams and microstructure of butt and filled weld

The parts of the transverse control arm consist of the S460MC (1.0982), S355MC (1.0976) and DD13 (1.0335) with sheet thicknesses between 2.5 and 7 mm. The critical region of failure and the resulting detail are located at the rear bearing tube (fig.3). The assembly is joined with an automatic MAG welding process. The stiffness of the coarse FE model is compared with the corresponding static loaded experiment by means of optical three dimensional deformation analysis and local strain measurements with strain gauges.

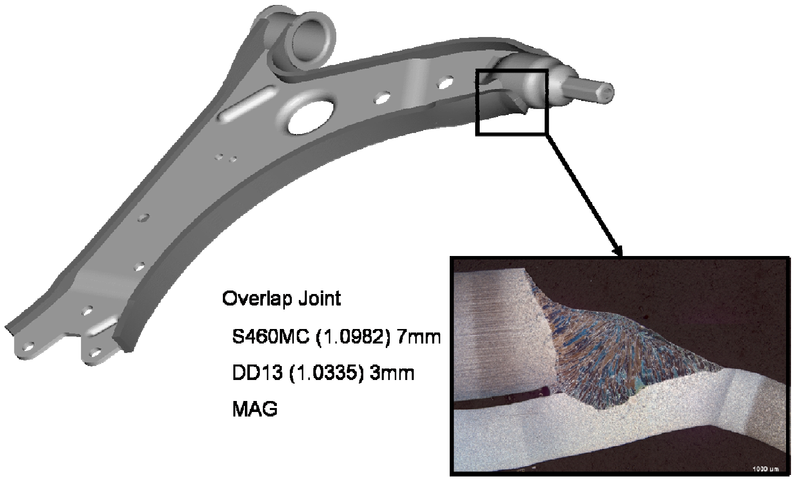

Figure 3. Component and region of failure for fatigue tests

After performing the stiffness alignment of the coarse model, a submodel of the region of failure is created. The real weld seam geometry is measured by means of laser-triangulation and used for modelling the weld seam in the submodel. The fictious notch rounding is performed with a notch radius $r_f = 0.05$mm (fig.4). Because of the presence of a heavily multiaxial stress state acting on the weld seams of the control arm the Mises strength criterion is used to determine the equivalent notch stress.

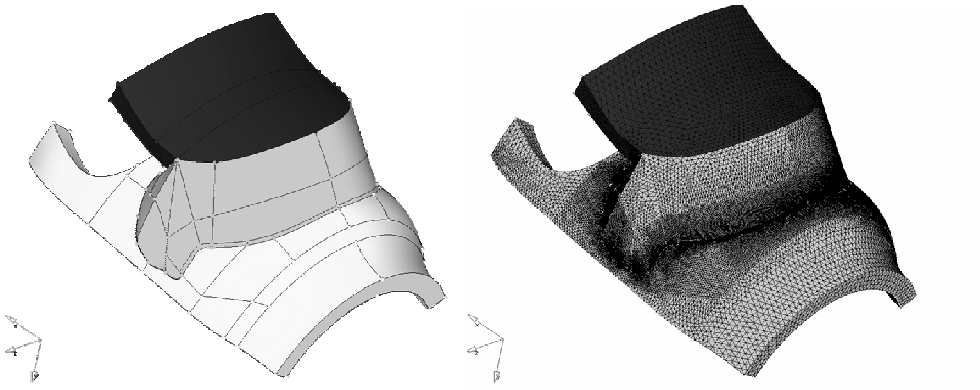

Figure 4. Submodel of the overlap joint with fictious notch radius r_f=1mm and r_f=0.05

First the transverse control arm is tested under dynamic alternating loading (R=-1) with constant amplitude. The end of the test is defined by the fracture of the component or by 10^7 numbers of cycles. In a further step the control arm is tested under variable amplitudes.

3 INCIPIENT CRACK DETECTION

During the load-controlled test with constant amplitude and pulsating load (R=0), the signal of three strain gauges were recorded. The strain gauges were located in a distance of 3 mm from the weld seam, witch is equal to the plate thickness in this area of the specimen. The distance between the strain gauges perpendicular to the load direction was 10 mm and the total width of the specimen was 41 mm. In fig. 5 is the strain amplitude versus the number of cycles shown. The strain gauge no. 3 shows a significant change in the strain amplitude after 200.000 cycles. The experiment was stopped after a 10 % change in strain amplitude.

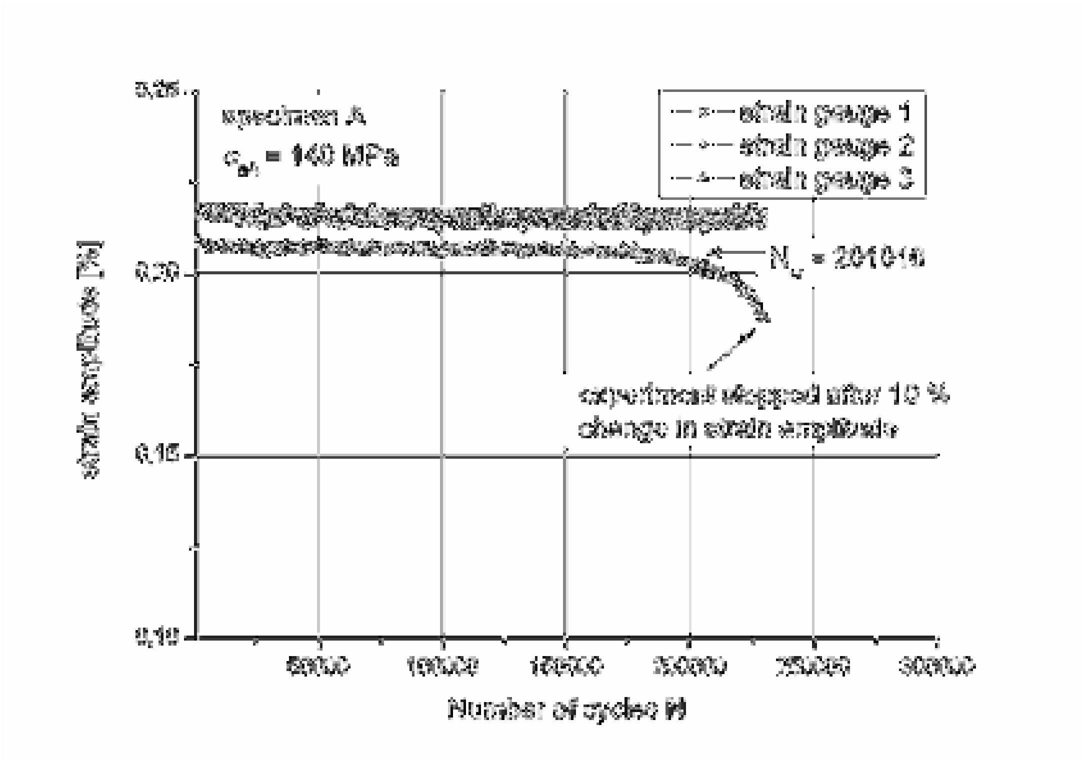

Figure 5. Incipient crack detection by strain gauges

In fig. 6 the fracture surface of specimen A after a 10 % change of the local strain amplitude is shown. For this purpose, the specimen was cooled with liquid nitrogen to produce a brittle fracture by load. Four different areas of fatigue crack surfaces were identified. The strain gauge no. 3 was located near the crack surfaces *c* and *d*. The fatigue crack surface at point *d* has a depth of about 1 mm at this time of the experiment.

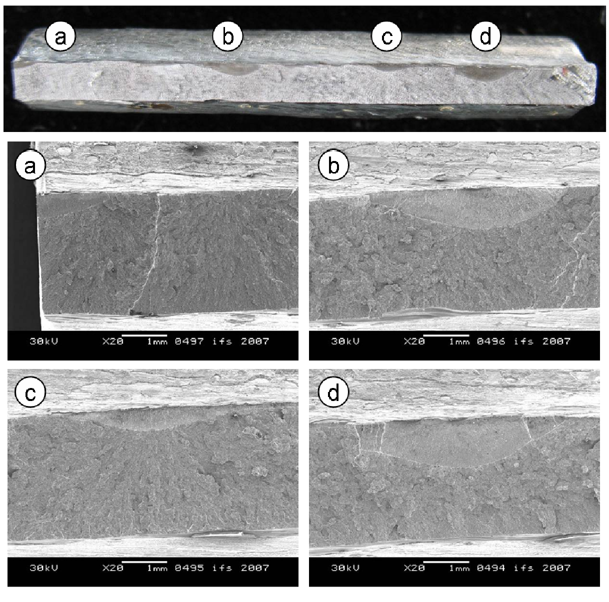

Figure 6. Fracture surface after 10 % change of local strain amplitude under dynamic loading

This investigation showed that, with the help of strain gauges, it is possible to detect the incipient crack, when the strain gauge is located near the fatigue crack. For example, the strain gauges no. 1 and no. 2 in figure 3 showed no significant changes in the strain amplitudes. The distances between the fracture and the strain gauges were too high. So the accuracy of this method depends on the geometry between the crack and the strain gauges.

A further possibility to get information about the incipient crack is given by the ultrasonic-burst-phase-thermography. In this research, a short outlook of this method is given. Fig. 7 shows a phase-image of a butt joint specimen after a 10 % change of strain amplitude. The dimension perpendicular to the load direction of the fatigue crack surface is identifiable. In contrast to the strain gauge method, the experiment must be stopped. For the ultrasonic-burst-phase-thermography an external experimental setup is necessary.

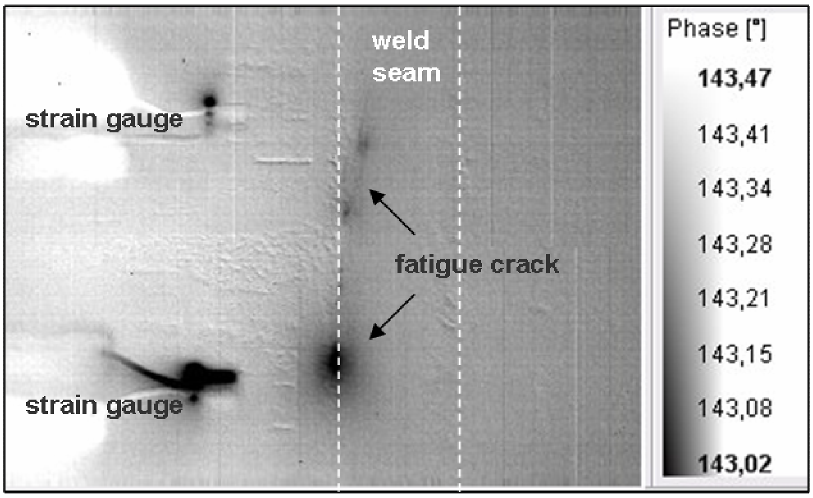

Figure 7. Thermography investigation of incipient crack detection

4 FINITE ELEMENT ANALYSE (FEA)

The numerical determination of the nominal, structural and notch stresses is performed with proper finite-element models. For a local approach, according to the notch stress analysis, a submodelling technique is used. Existing weld seam and specimen tolerances are included by the usage of parametric models. The FE models are compared with the corresponding experiment by means of an optical three dimensional deformation analysis and strain measurements with strain gauges. Fig. 8 shows the results (equivalent stress v. Mises) of the global FE-models of the tested specimens by a nominal tensile load of σ_a = 100 MPa. These solid models were the basis for the determination of nominal stresses and hot-spot stresses.

The models include the misalignment of weld edges concerning the different sheet thicknesses, which leads to an increase of load in one region of the weld seam. To calculate the hot-spot stresses, a linear extrapolation with the evaluation points 0.4 t and 1.0 t is chosen. The notch stresses are determined with the help of a submodelling technique. Fig. 9 shows the equivalent notch stresses (v. Mises) with the fictitious radius r_f = 1.0 mm. In course of the different geometry of the specimens and the different weld geometry, the notch stresses of specimen B are higher than that of specimen A.

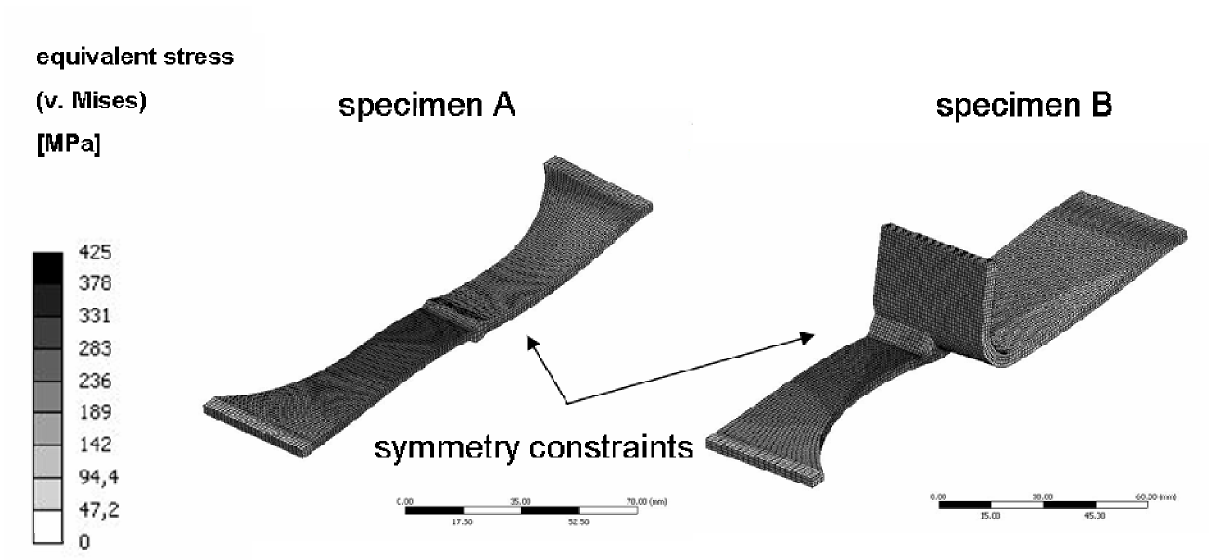

Figure 8. Results of the FE-globalmodels of butt (specimen A) und fillet (specimen B) joint

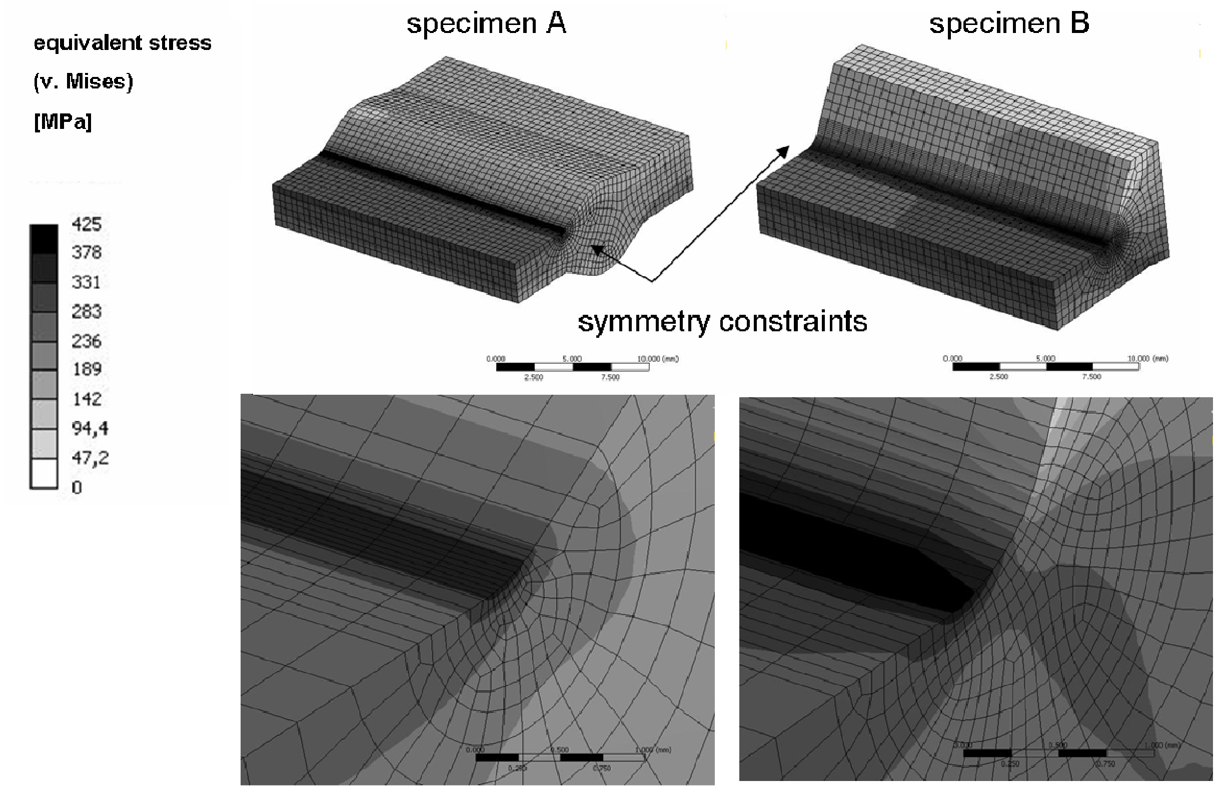

Figure 9. Results of the FE-submodels of butt (specimen A) und fillet (specimen B) joint with the fictitious radius r_f = 1.0 mm

In the comparison between the FE-models and the failure of the specimens in the experiments, the hot-spots lie at the same places.

5 RESULTS OF THE FATIGUE STRENGTH TESTS

The test results for the specimens with butt joint and with the combination of butt und fillet joint are shown in the nominal stress system in fig. 10. The misalignment of weld edges leads to an additional bending load. In this examination, a distinction was made between the fatigue life to crack initiation (technical crack depth a = 1.0 mm) and to final rupture. The results permitted an evaluation according to the concept of uniform SN-curve [1] with a appointed knee point at $N_k = 10^7$ cycles for both specimens, a uniform scatter of T_s = 1:1.24 (specimen A) and a uniform scatter of T_s = 1:1.30 (specimen B) and slopes of k = 7 - 8. For $N > N_k$ the slope of k* = 45 is derived by assuming a fatigue strength decrease of 5% per decade [3]. At the knee point, nominal stress amplitudes of $\sigma_{a,n}$ = 71 MPa for the butt joint and $\sigma_{a,n}$ = 72 MPa for the butt and fillet joint are obtained. To get more information between $10^6 < N < 10^7$, further test will be done.

The combined results of specimens A and B in a single SN-curve are shown in the hot spot stress and in the notch stress system in fig. 11.

The results also permitted an evaluation according to the concept of uniform SN-curve [1] with a appointed knee point at $N_k = 10^7$ cycles for both specimens, a uniform scatter of T_s = 1:1.27 and slopes of k = 8. For $N > N_k$ the slope of k* = 45 is derived by assuming a fatigue strength decrease of 5% per decade [3]. At the knee point, hot-spot stress amplitudes of $\sigma_{a,\,hs}$ = 208 MPa and notch stress amplitudes of $\sigma_{a,k}$ = 300 MPa for both connections are obtained. Concerning the notch stress concept, the results were obtained with a fictitious radius r_f = 1.0 mm.

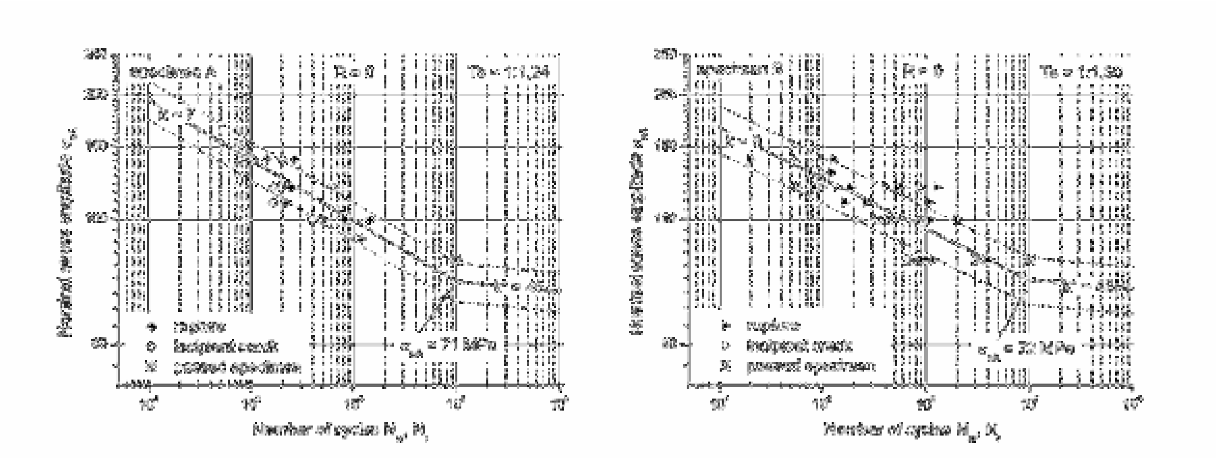

Figure 10. SN-curves of specimen A and B in the nominal stress system under pulsating loading

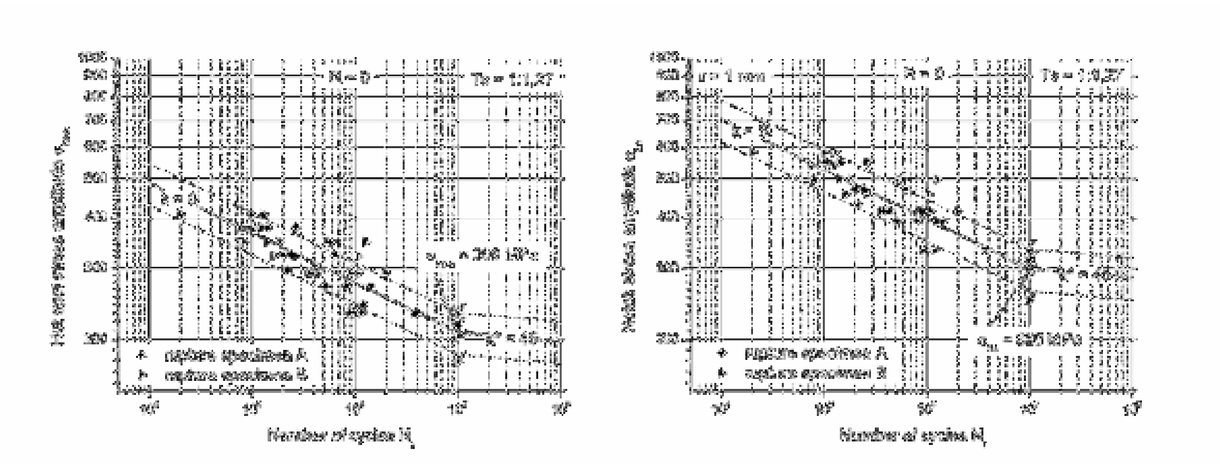

Figure 11. SN-curves of specimen A and B in the hot spot stress and notch stress system under pulsating loading

6 CONCLUSIONS

The investigation showed a good correlation between the calculated strains in the FE-models and the measured strains of the specimens with the help of strain gauges. Finally the calculated hot-spots are the areas of failure of the specimens in the experiments

When the strain gauge is located near the fatigue crack, the investigation showed that it is possible to detect the incipient crack. The ultrasonic-burst-phase-thermography is a further possibility to get information about the incipient crack.

The fatigue strength behaviour was determined with load-controlled test with constant amplitude and pulsating load of two different specimen types. It was possible to present the results in a single SN-curve in the nominal, hot-spot and notch stress system with a uniform scatter below $T_s = 1:1.50$ and slopes of $k = 8$ for $N < N_K$. Further investigations are the load-controlled test with constant amplitude and pulsating load with the described components (fig. 1). Afterwards a comparison between the fatigue strength of the components and the tested specimens will be possible.

7 ACKNOWLEDGEMENTS

The results presented here are developed in the context of the research cluster "applicability of fatigue design concepts for dynamic loaded weld structures" under the frame of the AiF (German Federation of Industrial Cooperative Research Associations "Otto von Guericke"). Subproject AiF 14519N ("Offene und geschlossene Stahlprofile aus dem Schienenfahrzeugbau") is supported by the DVS (Deutscher Verband für Schweißen und verwandte Verfahren e.V.), subproject AiF 14521N („Schutzgasgeschweißte Stahlstrukturen geringer Wanddicke aus dem Automobilbau") is promoted by the FOSTA (Forschungsvereinigung Stahlanwendung e. V). We thank the AiF for the financial support.

8 REFERENCES

[01] Hobbacher, A.: Fatigue Design of Welded Joints and Components. IIW-Doc. XIII – 1539 –96 / XV – 845 – 96, Cambridge, Abington (1996)

[02] FKM-Richtlinien „Rechnerischer Festigkeitsnachweis für Maschinenbauteile" und „Bruchmechanischer Festigkeitsnachweis. VDMA-Verlag, Frankfurt am Main (2002)

[03] Sonsino, C.M.; Maddox, S.J.: Multiaxial Fatigue of Welded Structures – Problems and Present Solutions. 6th International Conference on Biaxial/Multiaxial Fatigue and Fracture, Lisboa, Portugal, 25.-28.6.2001. Ed. European Structural Integrity Society (ESIS) Vol. I(2001), S. 3-15